remote sensing

MDPI

Article

Applicability of Relatively Low-Cost Multispectral Uncrewed Aerial Systems for Surface Characterization of the Cryosphere

Colby F. Rand and Alia L. Khan *

Department of Environmental Sciences, College of the Environment, Western Washington University, Bellingham, WA 98225, USA; randc@wwu.edu
* Correspondence: alia.khan@wwu.edu

Abstract: This paper investigates the ability of a relatively low cost, commercially available uncrewed aerial vehicle (UAV), the DJI Mavic 3 Multispectral, to perform cryospheric research. The performance of this UAV, where applicable, is compared to a similar but higher cost system, the DJI Matrice 350, equipped with a Micasense RedEdge-MX Multispectral dual-camera system. The Mavic 3 Multispectral was tested at three field sites: the Lemon Creek Glacier, Juneau Icefield, AK; the Easton Glacier, Mt. Baker, WA; and Bagley Basin, Mt. Baker, WA. This UAV proved capable of mapping the spatial distribution of red snow algae on the surface of the Lemon Creek Glacier using both spectral indices and a random forest supervised classification method. The UAV was able to assess the timing of snowmelt and changes in suncup morphology on snow-covered areas within the Bagley Basin. Finally, the UAV was able to classify glacier surface features using a random forest algorithm with an overall accuracy of 68%. The major advantages of this UAV are its low weight, which allows it to be easily transported into the field, its low cost compared to other alternatives, and its ease of use. One limitation would be the omission of a blue multispectral band, which would have allowed it to more easily classify glacial ice and snow features.

Keywords: remote sensing; snow algae; multispectral imagery; drones; UAVs; supervised classification; random forest; machine learning

Citation: Rand, C.F.; Khan, A.L. Applicability of Relatively Low-Cost Multispectral Uncrewed Aerial Systems for Surface Characterization of the Cryosphere. *Remote Sens.* **2024**, *16*, 3662. https://doi.org/10.3390/rs16193662

Academic Editors: Huaqiang Du and Ulrich Kamp

Received: 31 July 2024
Revised: 26 September 2024
Accepted: 28 September 2024
Published: 1 October 2024

1. Introduction

Global climate change is rapidly affecting polar and high alpine environments by accelerating the melting of glaciers and mountain snowpacks, reducing biodiversity, and altering how ecosystems function [1]. The study of these ecosystems is difficult due to their remoteness, the cost and time associated with traveling to these locations, the difficult and dangerous nature of traversing glacierized regions, and the technical mountaineering skills and equipment that are often needed for accessing study sites. Due to these challenges, the acquisition of data from remotely sensed sources, including satellites and uncrewed aerial vehicles (UAVs), is particularly well suited for the study of these environments. Although satellite imagery from platforms such as Landsat and Sentinel-2 are readily available, free to download, and have a relatively high revisit frequency, satellite imagery of the Earth's surface cannot be acquired under cloudy conditions, the imagery is often not of a high enough spatial resolution for the monitoring of small-scale features, and images of snow-covered terrain often suffer from oversaturation artifacts due to the high reflectivity of snow [2,3]. In contrast, UAVs can capture images of the Earth's surface under cloudy conditions if they are flown below the cloud ceiling, they can visualize features at the centimeter scale if flown at a low altitude, and they can be equipped with a variety of optical, multispectral, or thermal sensors depending on the goals of the survey [3,4].

Although commercially available UAVs or custom-built UAVs for research purposes have only recently emerged, the utilization of UAVs for cryospheric research has experienced a significant surge in the past decade [3,5]. These studies are wide ranging and have

utilized UAVs for a variety of purposes, including the mapping of glacier ablation in the North Cascades [6], the mapping of surface features of an alpine glacier in the Alps [7], the identification and characterization of biotic and abiotic components within penguin colonies on the Antarctic Peninsula [4], the estimation of snow depth from photogrammetric methods [8], and the quantification of albedo change from snow algae on a glacier in the Cascades [9]. These studies found UAVs to be a more viable and inexpensive option than satellite imagery or in situ ground observations. For a holistic review of over 100 studies utilizing UAVs for cryospheric research and a discussion of the latest methodological advancements, hardware and software improvements, results, and future prospects of such cryospheric studies, see the review, "Applications of Unmanned Aerial Vehicles in Cryosphere: Latest Advances and Prospects", published in the journal Remote Sensing in 2020 [3].

In this paper, we evaluate the applicability of the newly released (late 2022) DJI Mavic 3 Multispectral (hereafter referred to as the Mavic 3M) for cryospheric research. This equipment was designed and manufactured by DJI in Shenzen, China. Specifically, we investigate its ability to: (1) map the spatial and temporal distribution of red snow algae; (2) quantify snowmelt timing and suncup formation in an alpine basin; and (3) classify glacier surface features and monitor glacial ablation. Where applicable, the data products generated by the Mavic 3M are compared to the data products generated by a higher cost Micasense RedEdge-MX dual camera system, which was attached to a more expensive DJI Matrice 350 RTK UAV (hereafter referred to as the Matrice 350). This equipment was also designed and manufactured by DJI in Shenzen, China. The goal of this investigation is to assess the strengths and weaknesses of the Mavic 3M as a tool for glaciological research. This information should help inform other researchers who are interested in acquiring a UAV for their research on if this particular model is suitable for their study questions, or if they would benefit from a higher-cost system.

The performance of the Mavic 3M was tested at three study sites: the Lemon Creek Glacier within the southern extent of the Juneau Icefield in Alaska; Bagley Basin, an alpine basin to the northeast of Mt. Baker, Washington; and the Easton Glacier on the southern flank of Mt. Baker, Washington. A UAV mapping campaign of the Lemon Creek Glacier with the Mavic 3M and Matrice 350 was carried out over a three-day period from 21 August 2023, to 23 August 2023, with the primary goal of mapping the spatial distribution of red snow algae on the glacier's surface. Mavic 3M mapping surveys at Bagley Basin were carried out on 8 June, 26 June, 5 July, 10 July, 13 July, and 17 July 2023. The key goals of these surveys were to monitor the change in snow-covered extent as the snow melted in the basin and to analyze suncup formation on the snow surface. Mavic 3M mapping missions at the Easton Glacier were carried out on 20 July, 1 August, 13 August, and 8 September 2023. The primary goal of these surveys was to classify glacier surface features in the imagery using a supervised classification method.

Snow algae has been observed on snow surfaces within the Juneau Icefield and the North Cascades, including Mt. Baker [6,9,10]. Quantifying the spatial and temporal distribution of this algae is important because snow algae act to reduce snow albedo, thus increasing snowmelt [11–13]. This occurs because snow algae contain a photoprotective pigment called astaxanthin that protects the inside of the cell by absorbing incoming solar radiation and converting excess energy into heat [14]. This creates a "bioalbedo-feedback loop" that accelerates the melting of snow surfaces [15]. This feedback loop begins when excess heat absorbed by astaxanthin melts the surrounding snow grains, producing meltwater. Snow algae require liquid water and nutrients to grow, so this meltwater, alongside nutrients from air blown or local sources, facilitate algal growth. Increased algae concentrations then produce increased quantities of meltwater, and the cycle intensifies. The concentration of snow algae blooms can therefore be used as a proxy for snowmelt [16]. The mapping of snow algae from multispectral satellite imagery is possible through the application of various spectral indices [15–21] and machine learning

based image classification techniques [21–23]. These techniques can be applied to UAV imagery as well [9,24].

2. Materials and Methods

2.1. Study Sites

UAV mapping surveys with the Mavic 3M were carried out on the Lemon Creek Glacier within the Juneau Icefield, Alaska; Bagley Basin, an alpine basin in the Mount Baker Snoqualmie National Forest, Washington; and the Easton Glacier on the southern flank of Mount Baker, Washington (Figures 1 and 2).

2.1.1. Lemon Creek Glacier, Alaska

The Lemon Creek glacier is located at the southernmost extent of the Juneau Icefield in southeast Alaska (58.364°N, 134.350°W, Figure 1a). The mass balance of the Lemon Creek Glacier has been measured annually since the mid-1940s, making it the joint longest continuous record of glaciological measurements in North America. It is also the sole benchmark glacier for the World Glacier Monitoring Service and the United States Geological Survey in southeast Alaska [25]. The glacier has undergone extensive melting since measurements began, with its surface area shrinking from 12.8 km^2 in 1948 to 9.7 km^2 in 2018, alongside considerable thinning [25]. This glacier, and others within the Juneau Icefield, are known to have extensive red algae blooms growing on the surface in the summer months [10]. Our UAV mapping campaign at the Lemon Creek glacier focused on the southern half of the glacier since the snow on the northern half had already melted out to reveal the blue ice underneath, and the snow algae blooms were strongest toward the southernmost extent of the glacier.

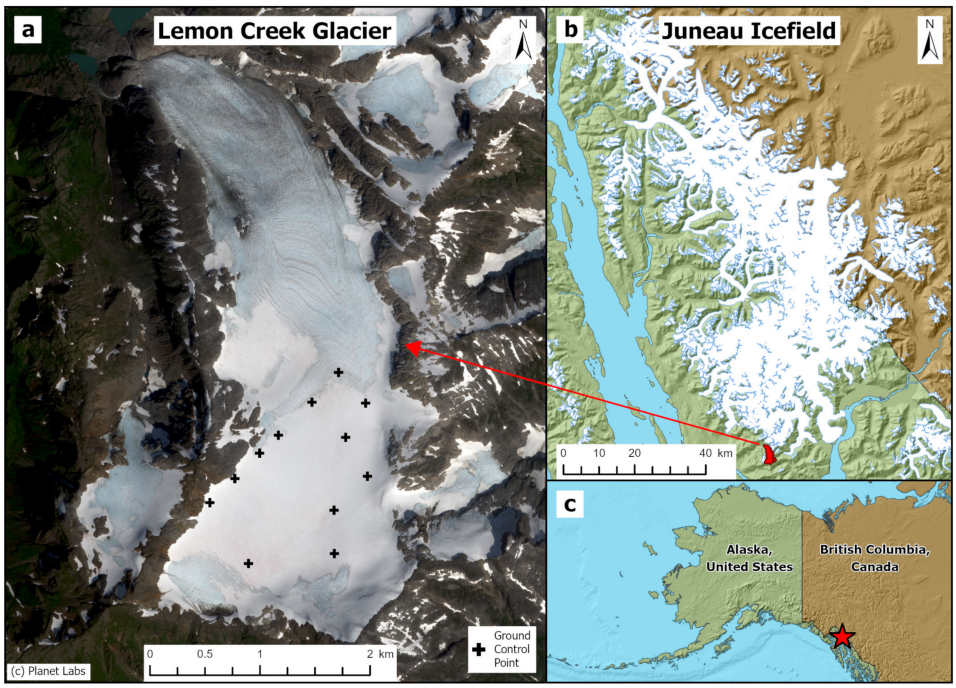

Figure 1. (**a**) SkySat image of the Lemon Creek Glacier (© Planet Labs). The locations of the ground control points used during this drone survey are shown by the black crosses. (**b**) The Lemon Creek glacier is located in the southernmost extent of the Juneau Icefield. Glaciated areas are shown in white (RGI Consortium [26]). (**c**) The Juneau Icefield is located on the border of southeast Alaska, USA and British Columbia, Canada, as shown by the red star. (Map projection: WGS 1984 UTM Zone 8N).

2.1.2. Bagley Basin, Washington

Bagley Basin is located in the Mount Baker-Snoqualmie National Forest, adjacent to the Mt. Baker Ski Area (48.854°N, 121.695°W, Figure 2c). The basin features two alpine lakes that are primarily fed by snowmelt. Upper Bagley Lake is the larger of the two lakes and is connected by a stream to Lower Bagley Lake, which flows into a tributary of the North Fork Nooksack River. The basin is mostly snow-covered until mid-summer and features a flat, marshy environment in the areas surrounding the lakes. The basin has steep, rocky sides that transport avalanched snow and debris down into the basin. Bagley Basin and the surrounding region receive an exceptionally high amount of snowfall each year. During the 1998–1999 winter, the nearby Mt. Baker Ski Area reported a record 1140 inches of snowfall, the official record for the most snowfall ever measured in a single season anywhere in the world [27].

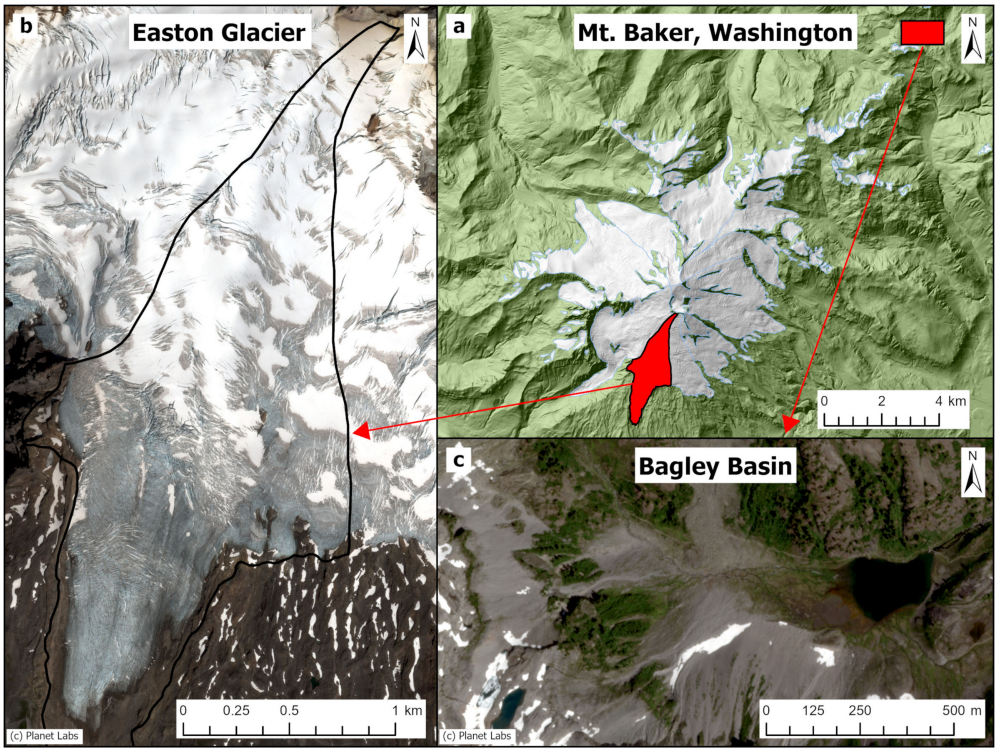

Figure 2. (**a**) Topographic reference map of Mt. Baker, Washington, USA, showing glaciated areas in white (RGI Consortium [26]). (**b**) SkySat image of the Easton glacier on the southern slope of Mt. Baker (© Planet Labs). The outline of the glacier is shown by the black polygon (RGI Consortium [26]). (**c**) SkySat image of Bagley Basin, an alpine basin to the northeast of Mt. Baker, adjacent to the Mt. Baker Ski Area (© Planet Labs). (Map projection: WGS 1984 UTM Zone 10N).

2.1.3. Easton Glacier, Washington

The Easton Glacier is located on the southern flank of Mt. Baker, Washington (48.740°N, 121.837°W, Figure 2b). The glacier has a total area of 2.87 km^2, its highest point is located at 2900 m a.s.l., and its terminus is located at 1680 m a.s.l. [28]. The annual mass balance of this glacier has been monitored every year since 1990 by the North Cascade Glacier Climate Project (NCGCP) [28]. These measurements reveal a strong negative mass balance of the Easton Glacier from 1990 to 2010, averaging −0.52 m w.e. a^{-1} (water equivalence). Terminus observations reveal a retreat of 320 m from 1979 to 2009 [29].

2.2. Drone Platforms and Instruments

2.2.1. DJI Mavic 3 Multispectral

Due to its compact size (223 × 96.3 × 122.2 mm folded) and weight (951 g), the Mavic 3M is highly portable and easy to transport in the field (Figure 3a). The aircraft has a maximum flight speed of 15 m/s in normal mode (21 m/s in sport mode) and a maximum flight time of 43 min (under ideal conditions). Omnidirectional obstacle sensing allows for accurate detection of obstacles in all directions, and real-time terrain-follow allows for aerial surveying to be performed in steep-sloped landscapes, all without needing external elevation data. It is equipped with an integrated 20MP 4/3 CMOS RGB camera and four 5MP multispectral sensors (Green: 560 ± 16 nm; Red: 650 ± 16 nm; Red Edge: 730 ± 16 nm; Near Infrared: 860 ± 26 nm). It has a built-in spectral sunlight sensor that detects solar irradiance in real time to obtain more accurate band reflectivity, which improves the consistency of data collected in different regions, weather conditions, and times [30]. The aircraft is equipped with a Real Time Kinematic (RTK) module on top of its body that can communicate directly with a Global Navigational Satellite System (GNSS) base station to provide centimeter-level RTK positioning. As of July 2024, the MSRP for this device was $4618 USD.

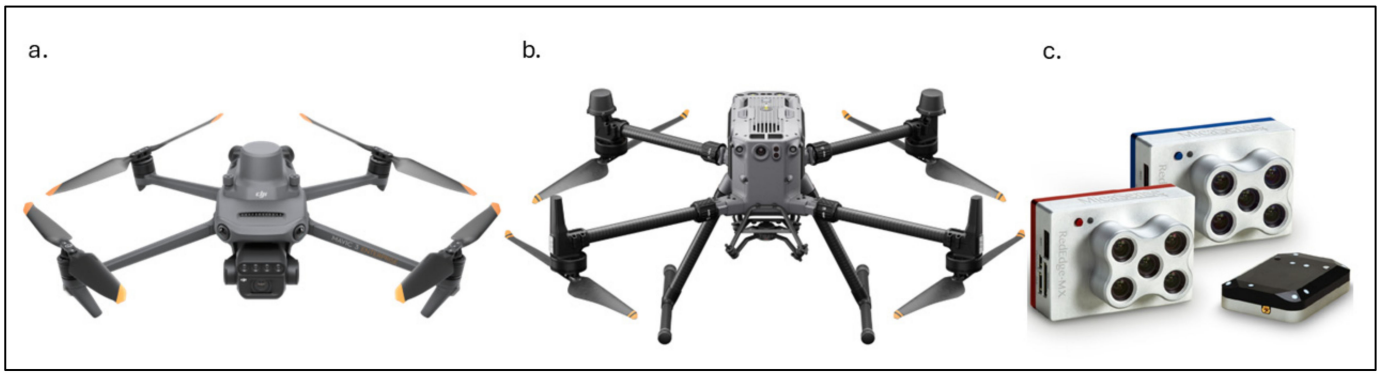

Figure 3. Drone platforms and sensors. (**a**) DJI Mavic 3 Multispectral (Mavic 3M), (**b**) DJI Matrice 350 RTK (Matrice 350), (**c**) Micasense RedEdge-MX Multispectral Dual-Camera System (Micasense) and downwelling light sensor (DLS).

2.2.2. DJI Matrice 350 RTK

The Matrice 350 is DJI's flagship enterprise drone engineered for professional-grade industrial tasks (Figure 3b). Although the base model of this drone does not come equipped with an external camera, it supports a maximum payload capacity of 2.7 kg, allowing for a wide variety of sensors to be attached. In this study, we attached a Micasense RedEdge-MX Multispectral dual-camera system to the bottom of the UAV. Due to its larger size (430 × 420 × 430 mm folded) and weight (6.47 kg), this drone is more difficult to bring into the field or carry to remote field sites. The aircraft has a maximum flight speed of 23 m/s and a maximum flight time of 55 min (under ideal conditions and no payload). A six-directional binocular vision system and an infrared sensing system provides six-directional awareness, positioning, and obstacle-sensing for comprehensive protection during flight. Through the importation of a digital elevation model, the UAV supports terrain follow during flight to maintain a constant elevation above ground level. The drone is equipped with a night-vision FPV camera, which allows safe operation at night. The aircraft is equipped with an RTK module on top of its body that can communicate directly with a GNSS base station to provide centimeter-level RTK positioning. As of July 2024, the MSRP for this device with two batteries and the battery charging station was $11,729 USD.

2.2.3. Micasense RedEdge-MX Multispectral Dual-Camera System

The Micasense RedEdge-MX Multispectral Dual-Camera System is a 10-band camera system that captures surface reflectance in the coastal blue (222 nm), blue (475 nm), green (531 and 560 nm), red (650 and 668 nm), red edge (705, 717, and 740 nm), and NIR (842 nm) wavelengths. The sensor has a resolution of 1280 × 960, a 47.2 degree horizontal field of view, an output bit depth of 12-bits, and can capture a ground sample distance (GSD) of 8 cm/pixel per band when flown from an elevation of 120 m above ground level (a.g.l.). The sensors feature a global shutter and can capture images at a rate of 1 image per second. The total payload is 508.8 g. The camera system can be combined with a downwelling light sensor (DLS) for accurate ambient light calibration (Figure 3c). As of July 2024, the MSRP for this device was $8565.

2.3. UAV Mapping Protocol

All UAV flights conducted throughout this study adhered to the regulations outlined by the Federal Aviation Administration's (FAA) Part 107 guidelines. UAV operations were carried out by scientists who possessed a valid Small Unmanned Air System (Part 107) remote pilot certification. Concurrent with FAA regulations, the maximum flight height was set to 120 m above ground level (AGL), the UAVs were not flown directly over people or buildings, and the UAVs always remained within line-of-sight of the pilot. The Lemon Creek glacier study area is located within Class G uncontrolled airspace, and as such, did not require any special permission to fly a drone at. This area is popular for helicopter tourism, however, so extreme caution was taken when other crewed aircraft were flying in the immediate vicinity. Both the Easton Glacier and Bagley Basin are outside of the Mt. Baker Wilderness area, so no special permission was required to fly there. Most of Easton Glacier is located within the Mt. Baker National Recreational Area, where motorized vehicles (including drones) are permitted. Because if its proximity to the Mt. Baker Ski Area, motorized vehicles are also permitted at Bagley Basin. Additionally, we had reached out to the U.S. Forest Service, and they granted us permission to fly in both areas without needing a special permit.

To improve the geolocation accuracy of the UAV surveys, the RTK modules on both UAVs were connected to an Emlid Reach RS2+ survey-grade GNSS receiver, which was placed on a tripod near each survey area to serve as a GNSS base station. This device was placed in an open area where it a clear view of the sky with as few obstructions on the horizon as possible. The device was set to average for 15 min to determine its position, then it was connected to the remote controller via Wi-Fi, which allowed the remote controller to relay GNSS corrections to the UAV during flight.

During the Bagley Basin and Lemon Creek Glacier flights, ground control points (GCPs) were laid across the survey area and tagged with a roving Emlid Reach RS2+ receiver to calculate their positions. When the roving receiver was connected to the base station receiver over LoRa radio, the locations of the GCPs could be tagged with centimeter-level precision. At Bagley Basin, 6 GCPs were evenly spread across the basin during each survey, although the location of each set of GCPs changed during each survey at Bagley Basin. At the Lemon Creek glacier, 12 GCPs were evenly spread across the surface of the glacier (Figure 1a). The locations of these GCPs were used to refine the geolocation accuracy of the orthomosaic and digital elevation models produced. At the Easton glacier, no GCPs were used for safety reasons, as that would have required traversing heavily crevassed regions of the glacier terminus.

All flight mission planning was carried out within the DJI Pilot 2 application on the UAV's remote controller. Flight parameters were set depending on the objectives of the survey, the given time restraints, and battery limitations. These parameters include the flight altitude, flight speed, front and side overlap, shot interval, and terrain follow. The parameters used during each UAV flight can be found in Appendix A.

The total flight time for the Lemon Creek glacier survey was approximately 10 h for both the Mavic 3M and the Matrice 350. Due to changing weather conditions, the images

for this survey were captured at various times over a three-day period from 21 August 2023 to 23 August 2023. Images were captured between the hours of 9 a.m. and 5 p.m. local time. The total flight time for the Bagley Basin surveys lasted between 1 to 3 h, depending on the size of the area surveyed. These images were captured between the hours of 9 a.m. and 4 p.m. local time. The total flight time for the Easton Glacier surveys lasted between 4 to 6 h, depending on the size of the area surveyed. These images were captured between the hours of 11 a.m. and 4 p.m. local time.

2.4. Orthomosaic and Digital Elevation Model Generation

All photogrammetric processing of UAV imagery was carried out within Agisoft Metashape Pro, Version 2.1, which allowed for the creation of 3D point clouds and geo-referenced DEMs and orthomosaics [31]. When processing Mavic 3M imagery, the RGB and multispectral images were processed in separate chunks due to their differing camera properties. The RGB images were added as single cameras, whereas the multispectral images were added as a multi-camera system, which allowed for all 4 spectral bands from the Mavic 3M camera, or all 10 spectral bands from the Micasense camera, to be grouped together. The reflectance of all multispectral images was calibrated using the downwelling light sensor attached to the top of both UAVs. An additional calibration for the Micasense images was carried out using images of the spectral reflectance panel captured by the Micasense camera before and after each flight. The survey images were then aligned with high accuracy, general preselection was enabled, the key point limit was set to 40,000, the tie point limit was set to 4000, and adaptive camera model fitting was enabled. After the images were aligned and a sparse point cloud was created, the cameras were optimized. If ground control points (GCPs) were used, they were imported from a CSV file, and new markers were created for each GCP. The GCPs were then manually marked in at least 10 images, and camera positions were optimized again. A dense point cloud was then created using high quality and moderate depth filtering. A DEM was created using the point cloud as the source data, and the projection was set to the region's local UTM zone (WGS 1984 UTM zone 10N for Mt. Baker, WA and WGS 1984 UTM zone 8N for the Lemon Creek Glacier, AK). An orthomosaic was generated using the DEM as the surface. The Set Raster Transform tool was used to normalize the multispectral data range from 0–1 by dividing each band by 32,768 (the input bands are 16-bit integers, but the 100% reflectance for each band corresponds to the middle of the available range, i.e., to 32,768, or 2^{15}). The DEMs and orthomosaics were exported as TIFF files, and the multispectral orthomosaics had their raster transform parameter set to index value so that the reflectance value was output between 0–1 for each pixel. The spatial resolution of each orthomosaic and flight parameters for each survey are listed in Table A1 in Appendix A. Additional details regarding the accuracy metrics for the orthomosaics and all Agisoft Metashape parameters used during the Structure from Motion process can be found in the Supplemental Materials.

Before any analysis was conducted on the Mavic 3M and Micasense orthomosaics from the Lemon Creek glacier, these rasters were clipped to the same survey extent in the southern region of the glacier so that their results could be directly compared. The total area of this clipping extent was 18,950 m^2. The southern region of the Lemon Creek glacier was used to compare the two sensors since this area was included in both UAV mapping missions, there was a high concentration of red snow algae in this region, and there was no rock and very little blue ice which could complicate the classification.

2.5. Mapping Snow Algae with Spectral Indices

The detection and mapping of snow algae from remotely sourced imagery can be accomplished through the application of a spectral index that calculates the relative difference in surface reflectivity between the red and green bands of a given sensor [16,18–20]. When applied to snow-covered areas, this index calculates the presence/absence of red snow algae on a per pixel basis depending on whether the index's value is above or below a given threshold value. These index values have proven to be linearly correlated with

algal concentrations, allowing for the quantification of biomass over entire study sites if the algal concentrations at various index values are known [20]. One implementation of this index is the Optimized Red Green (ORG) index:

$$\mathrm{ORG} = \frac{R_{red} - 0.015}{1.02 \times R_{green}} > 1.0 \quad (1)$$

where R_{red} is the surface reflectivity in the red wavelengths and R_{green} is the surface reflectivity in the green wavelengths [6]. Pixels with an ORG index value > 1.0 are classified as containing snow algae, and pixels with an ORG index value < 1.0 are classified as algae-free. This index is a slight variation of the more simplified red/green band ratio and was specifically calibrated for mapping snow algae within Bagley Basin, WA using the Micasense camera system [6]. For this reason, this index was applied to Micasense and Mavic 3M multispectral orthomosaics of the Lemon Creek Glacier within ArcGIS Pro V3.3.1 to map the spatial distribution of algae across the glacier's surface.

While the default implementation of the ORG index assumes a threshold value of 1.0, as per Equation (1), different camera sensors may capture different amounts of light depending on the structural characteristics of the sensors themselves and the exposure settings. Thus, the ratio between the amount of light captured by the red and green bands may differ across various sensors. Furthermore, the classification of "algae" vs. "non-algae" was somewhat subjective since there was undoubtably some concentration of snow algae across the entire study area in the southern region of the Lemon Creek glacier. We therefore choose to only classify bright red blooms as "algae" since that was what was observable in the imagery. For these reasons, a different threshold value was used when classifying algae in the Mavic 3M and Micasense orthomosaics of the southern region of the Lemon Creek glacier. While a threshold value of 1.0 was tested on both rasters, this value strongly underestimated the amount of red snow algae in the Mavic 3M orthomosaic, and this value overestimated the amount of red snow algae in the Micasense orthomosaic. Various other threshold values were tested to obtain a more accurate classification. For the Mavic 3M orthomosaic, an ORG threshold value of 0.65 was selected, and for the Micasense orthomosaic, an ORG threshold value of 1.08 was selected.

After the UAV surveys at the Lemon Creek were conducted, 30 snow algae samples were collected from the southern region of the Lemon Creek glacier for another study associated with this field campaign. These sampling points were used here to assess the accuracy of the ORG index since these points were verified to contain algae. The total accuracy for each classification was calculated as the number algae samples that intersected with the ORG index divided by the total number of samples.

2.6. Supervised Classification of Snow Algae

Snow algae blooms on the Lemon Creek Glacier were also mapped using a random forest supervised classification method as a comparison to the spectral index method. A training dataset of polygons was created for 2 distinct classes: red snow algae and clean snow. A minimum of 20 training polygons were created for each class. These polygons were then input into the random trees classifier within ArcGIS V3.3.1 to classify the Mavic 3M and Micasense orthomosaics. The maximum number of trees was set to 50, the maximum tree depth was set to 30, and the maximum number of samples per class was set to 1000. Once classified, the total algae covered area within the Mavic 3M and Micasense orthomosaics was calculated.

As with the ORG method, the 30 snow algae samples that were collected from the southern region of the Lemon Creek glacier were used to assess the accuracy of the random forest classification. The total accuracy for each classification was calculated as the number of algae samples that intersected with the random forest classification divided by the total number of samples.

2.7. Monitoring Snowmelt and Suncup Formation

Changes in snow-covered extent and suncup morphology at Bagley Basin, Mt. Baker, were assessed through repeat UAV mapping surveys, resulting in the creation of orthomosaic images and digital elevation models (DEMs). Visual analysis revealed the timing of ice-out in Upper Bagley Lake and the complete removal of snow within Bagley Basin. The diameter of suncups were measured on the orthomosaic images using the measure tool within ArcGIS Pro V3.3.1 to evaluate changes in suncup size.

2.8. Glacier Surface Characterization

The 13 August 2023, Mavic 3M orthomosaic was input to a random forest supervised classification algorithm. A training dataset of polygons was created for 4 unique spectral classes: snow, ice, rock and heavy debris, and crevasse. A minimum of 20 training polygons was created for each class. This training dataset was input to the random trees algorithm within ArcGIS Pro V3.3.1 to classify the image. The maximum number of trees was set to 50, the maximum tree depth was set to 30, and the maximum number of samples per class was set to 1000. The Zonal Statistics tool was used to calculate the area of each spectral class.

To validate and assess the accuracy of this classification, 800 accuracy assessment control points (200 per spectral class) were created within ArcGIS Pro using the equalized stratified random method. This ensured a representative sample of points from all four spectral classes. Each control point was given a ground truth value by zooming in on the orthomosaic image to visually assign a spectral class. A confusion matrix, the overall accuracy, the Cohen's Kappa, as well as user's and producer's accuracies, were then calculated for this classification within R V.4.4.0 using the "caret" package.

3. Results

3.1. Case Study 1: Mapping Red Snow Algae, Lemon Creek Glacier, Juneau Icefield, Alaksa

A three-day mapping survey of the Lemon Creek Glacier was conducted from 21–23 August 2023, using both the Mavic 3M and the Matrice 350, equipped with the Micasense camera system. Both UAVs captured thousands of images of the glacier's surface, and the images were stitched together within Agisoft Metashape Pro to produce true color orthomosaic images (Figure 4) and multispectral composite orthomosaic images. Due to time constraints, the area mapped by the Mavic 3M was slightly larger than that mapped by the Micasense camera on the Matrice 350.

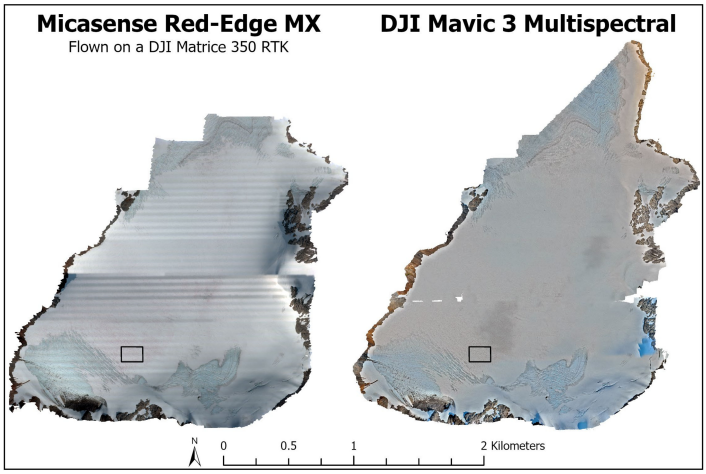

Figure 4. Orthomosaic images of the Lemon Creek Glacier, Juneau Icefield, Alaska, derived from images captured by the RGB bands (Band 5: Red-668, Band 3: Green-560, and Band 2: Blue-475) of the Micasense RedEdge-MX dual camera system (**left**) and the RGB camera on a DJI Mavic 3 Multispectral (**right**) collected from 21 August through 23 August 2023. The black rectangle toward the southern end of the Lemon Creek glacier depicts the high density algae area used for analysis in Figure 5. (Map projection: WGS 1984 UTM Zone 8N).

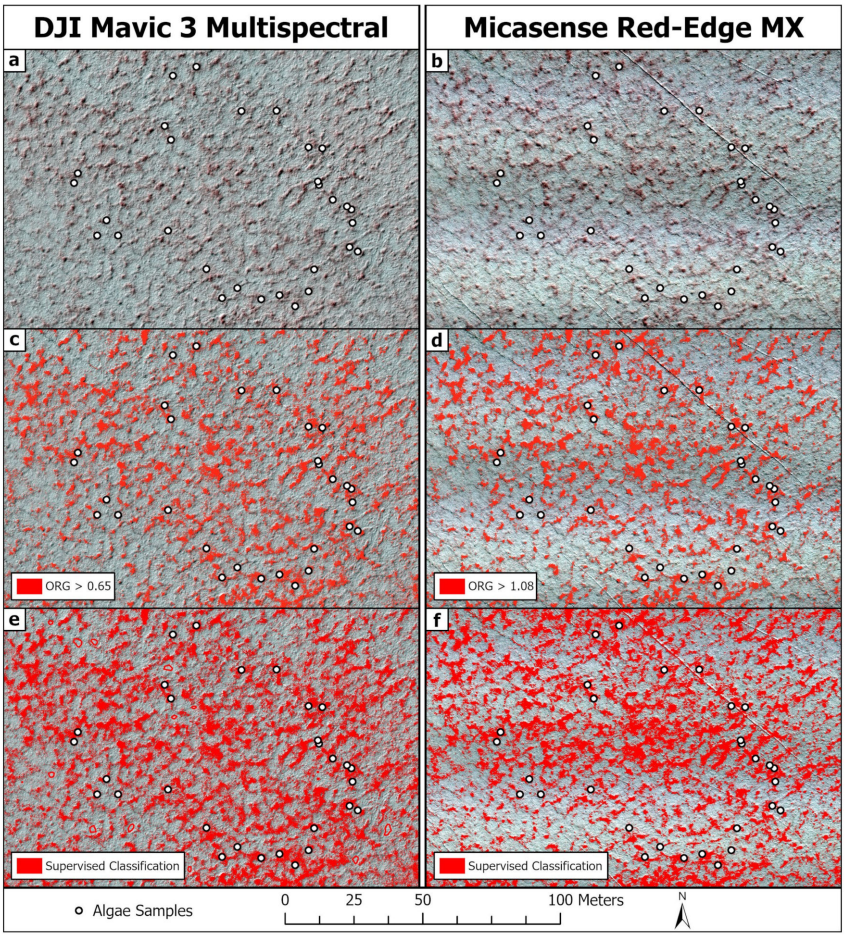

Figure 5. High density algae area in the southern region of the Lemon Creek Glacier, captured by the DJI Mavic 3 Multispectral, as shown in the left column, and Micasense Red-Edge MX camera system, as shown in the right column. (**a**) Mavic 3M multispectral composite orthomosaic, symbolized by Red: Band 2, Green: Band 1, and Blue: Band 1. Since there is no blue multispectral band on the Mavic 3M, the green band was used for both the green and blue symbology. (**b**) Micasense multispectral composite orthomosaic, symbolized by Red: Band 5, Green: Band 3, and Blue: Band 2. (**c**) ORG index applied to Mavic 3M orthomosaic. (**d**) ORG index applied to Micasense orthomosaic. (**e**) random forest classification of Mavic 3M orthomosaic. (**f**) random forest classification of the Micasense orthomosaic. Algae sample locations are shown by the black and white circles. (Map projection: WGS 1984 UTM Zone 8N).

The spatial distribution of red snow algae in the southern region of the Lemon Creek glacier was mapped by applying the ORG index and a random forest supervised classification algorithm to the Mavic 3M and Micasense multispectral composite orthomosaic images (Figure 5).

When the ORG index was applied, the total area classified as red snow algae was comparable across both orthomosaics (Table 1). In the Mavic 3M orthomosaic, the ORG index calculated the spatial extent of red snow algae to be 3083 m^2. In the Micasense orthomosaic, the ORG index calculated the spatial extent of red snow algae to be 3060 m^2. The random forest supervised classification approach resulted in similar results to the spectral index approach (Figure 4), although the area classified as red snow algae was greater for the supervised classification (Table 1). In the Mavic 3M orthomosaic, the random forest algorithm calculated the spatial extent of red snow algae was to be 5182 m^2. In the Micasense orthomosaic, the random forest algorithm calculated the spatial extent of red snow algae to be 5725 m^2.

Table 1. Total area classified as red snow algae in the southern region of the Lemon Creek glacier. Predicted algal extent was calculated by applying both the ORG index and a random forest supervised classification algorithm to the Mavic 3M and Micasense RedEdge-MX orthomosaic images.

Sensor	Classification Method	Classified Algal Extent	Accuracy
Mavic 3M	ORG > 0.65	3083 m^2	83%
Micasense RedEdge-MX	ORG > 1.08	3060 m^2	97%
Mavic 3M	Random forest	5182 m^2	93%
Micasense RedEdge-MX	Random forest	5725 m^2	100%

The accuracy of each classification was calculated by dividing the number of algae samples that intersected with each of the classifications by the total number of algae samples. For the Mavic 3M, the classification accuracy of the ORG index was 83% and the classification accuracy of the random forest classifier was 93%. For the Micasense orthomosaic, the classification accuracy of the ORG index was 97% and the classification accuracy of the random forest classifier was 100% (Table 1).

3.2. Case Study 2: Assessing Snowmelt Timing and Changes in Suncup Morphology at Bagley Basin, Washington

Bagley Basin was mapped with the Mavic 3M on 8 June, 26 June, 5 July, 10 July, 13 July, and 17 July 2023. The first flight provided a baseline to evaluate the timing of snowmelt and changes to suncup morphology throughout the early summer. The RGB orthomosaic from this first flight is shown in Figure 6. On this date, most of the basin was still snow covered and suncups were visible on all snow surfaces. Upper Bagley Lake was still frozen over, but the outline of the lake was visible by the light blue meltwater present around the periphery of the lake. Large, meltwater-filled suncups were present on the snow surface on top of the lake, as shown by the inset map in Figure 6. Upper Bagley Lake had completely melted out by the UAV flight on 5 July 2023.

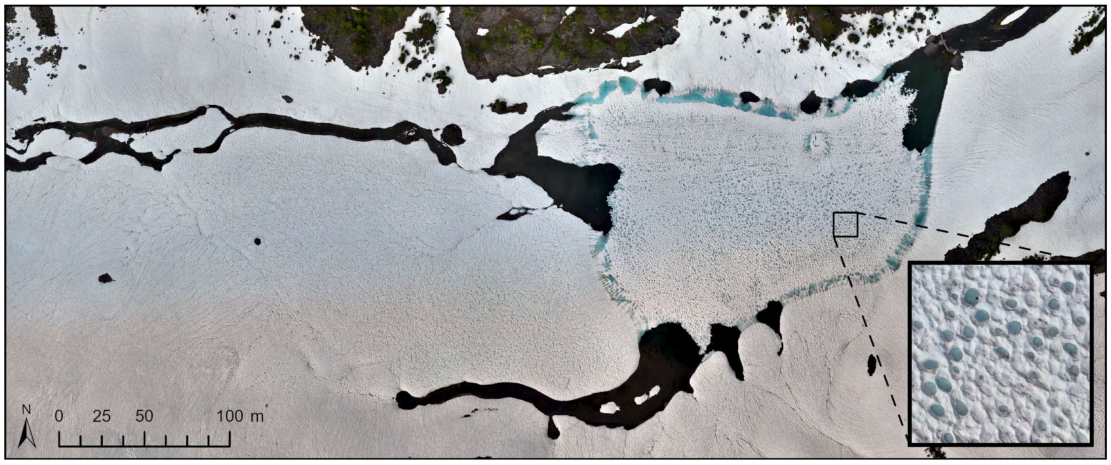

Figure 6. RGB orthomosaic of Bagley Basin, captured by the Mavic 3M on 8 June 2023. The inset map shows meltwater filled suncups on the surface of Upper Bagley Lake. (Map projection: WGS 1984 UTM Zone 10N).

RGB orthomosaics and DEMs of a snow-covered area to the west of Upper Bagley Lake show the visual change in suncup morphology throughout the early summer season (Figure 7). This area remained fully snow-covered during flights conducted on 8 June (Figure 7a, 26 June (Figure 7b), and 5 July 2023 (Figure 7c). On 10 July 2023 (Figure 7d), meltwater had begun to pool within the suncups, and by 13 July 2023 (Figure 7e), many

of the larger suncups had melted out completely, revealing the bare ground beneath. By 17 July 2023 (Figure 7f), the snow had completely melted from this area.

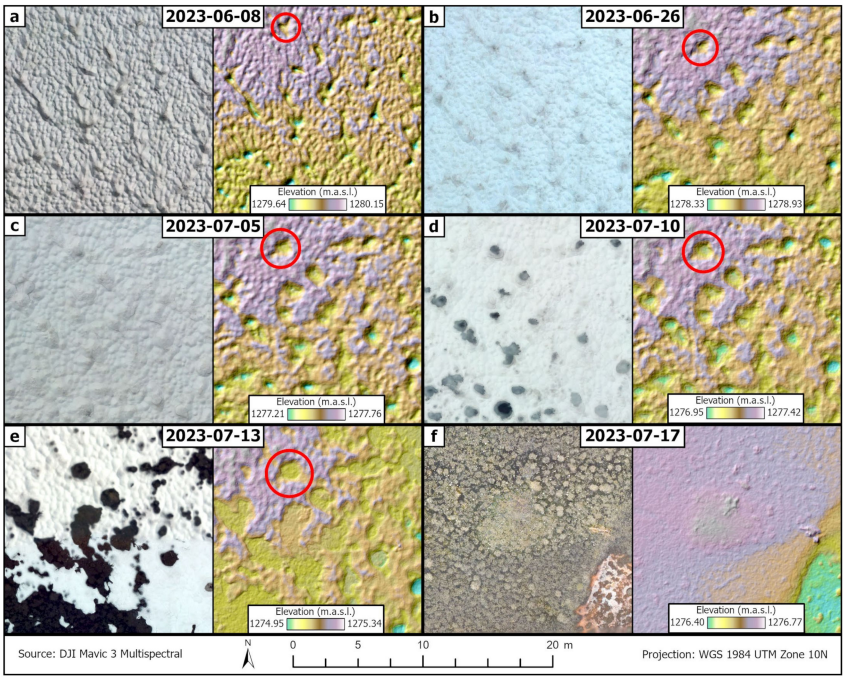

Figure 7. RGB orthomosaics and DEMs of a snow surface to the west of Upper Bagley Lake, within Bagley Basin, derived from DJI Mavic 3M imagery captured on (**a**) 8 June 2023, (**b**) 26 June 2023, (**c**) 5 July 2023, (**d**) 10 July 2023, (**e**) 13 June 2023, and (**f**) 17 July 2023. The red circle denotes an individual who's diameter was measured to assess changes to suncup morphology.

Over this period, the suncups in Bagley Basin are observed to have grown in diameter, with multiple smaller suncups coalescing to form one larger suncup. The red circle in Figure 6 tracks the changes to an individual suncup that is visible in all the flights, excluding the 17 July flight, when the snow had completely melted. On 8 June (Figure 7a), this suncup had an approximate diameter of 0.70 m. This had grown to 0.85 m on 26 June (Figure 7b), 1.20 m on 5 July (Figure 7c), 1.50 m on 10 July (Figure 7d), and 1.70 m on 13 July (Figure 7e), before the snow completely melted by 17 July (Figure 7f).

3.3. Case Study 3: Classification of Glacier Surface Features, Easton Glacier, Mt. Baker, Washington

Digital elevation models (DEMs) and orthomosaic images from repeat Mavic 3M flights over the Easton Glacier on 20 July, 8 August, 13 August, and 8 September 2023, show the retreat of the glacier's terminus and the opening of crevasses as the snow cover melts. (Figures 8 and 9). A progressively larger area was mapped with each consecutive flight as the methods were refined and additional batteries were purchased, extending the maximum flight duration. Due to the inaccessibility of the glacier at the height of the summer, GCPs were not used, limiting our ability to detect a change in surface elevation. The future use of GCPs could ameliorate this issue [9].

Based on a random forest supervised classification of the 13 August 2023, orthomosaic image, ice covered the greatest area within the clipped glacier extent at 802,947 m^2, or 49.8% of the total glacierized area (Table 2). Snow covered the second largest area at 637,576 m^2, or 39.6% of the total glacierized area (Table 2). Rock and heavy debris covered 144,553 m^2, or 9.0% of the total glacierized area (Table 2). Finally, crevasses covered 26,891 m^2, or 1.7% of the total glacierized area (Table 2).

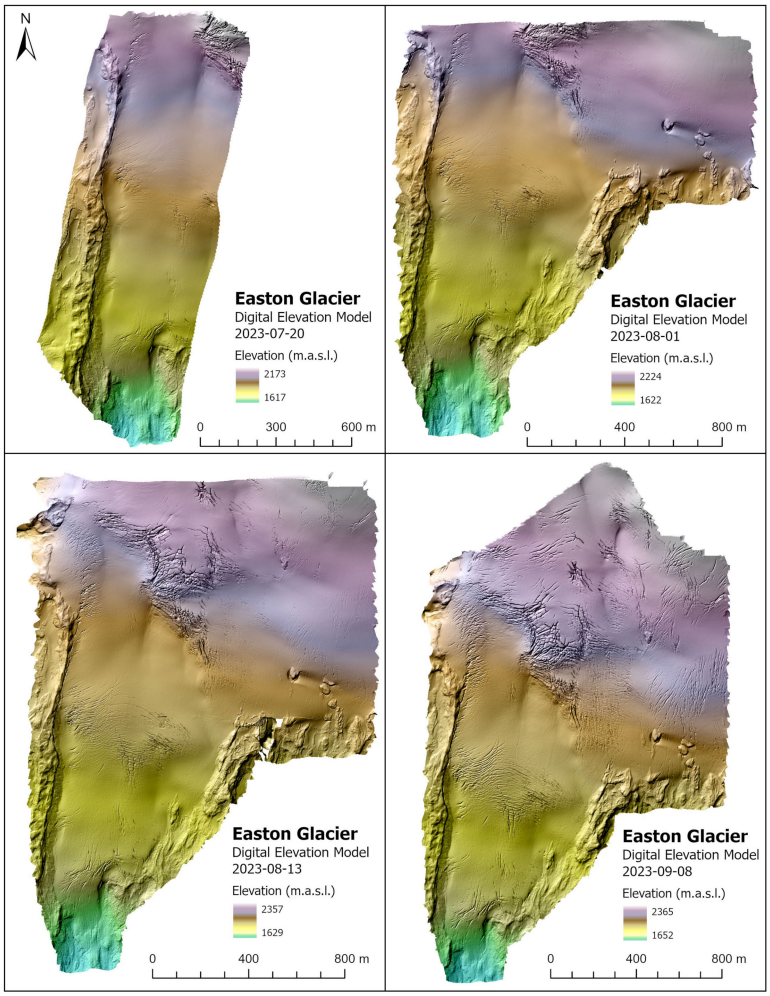

Figure 8. Digital elevation models of Easton glacier, captured by Mavic 3M mapping surveys on 20 July, 1 August, 13 August, and 8 September 2023. (Map projection: WGS 1984 UTM Zone 10N).

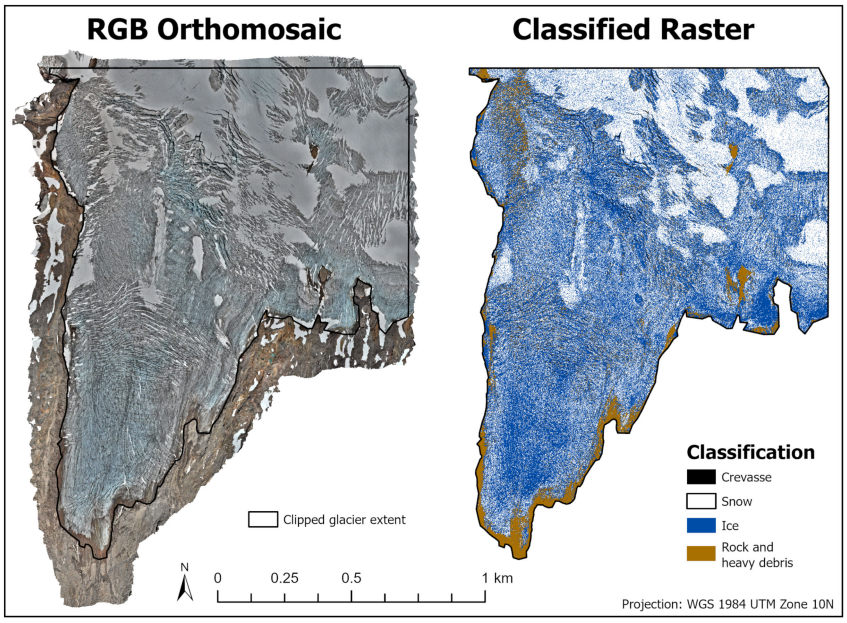

Figure 9. RGB orthomosaic and random forest supervised classification results of the 13 August 2023, Mavic 3M flight of the Easton glacier.

Table 2. Surface area of the 4 spectral classes from the random forest supervised classification of the 13 August 2023 Mavic 3M flight of the Easton glacier.

Spectral Class	Area	Percent of Total Area
Snow	637,576 m^2	39.6%
Ice	802,947 m^2	49.8%
Rock and Heavy Debris	144,553 m^2	9.0%
Crevasse	26,891 m^2	1.7%
Total	1,611,967 m^2	100%

The overall accuracy of this classification was 69%. The Cohen's kappa statistic was 0.5929. Additional information on the classification accuracy of each spectral class, including the user's and producer's accuracies, is shown in the confusion matrix in Table 3.

Table 3. Confusion matrix for the supervised classification of the 13 August 2023, DJI Mavic 3M orthomosaic of the Easton Glacier.

		Actual Class				
		Crevasse	Ice	Rock	Snow	User's Accuracy
Predicted Class	Crevasse	**159**	2	39	0	0.80
	Ice	1	**154**	6	38	0.77
	Rock	7	41	**143**	9	0.72
	Snow	0	98	3	**99**	0.50
	Producer's Accuracy	0.95	0.52	0.75	0.68	

4. Discussion

The Mavic 3M and the Matrice 350, equipped with the Micasense camera system, are both viable platforms to use when conducting cryospheric research. The Mavic 3M benefits from a lighter weight (951 g vs. 6.47 kg) and size (223 × 96.3 × 122.2 mm folded vs. 430 × 420 × 430 mm folded), making it much easier to transport to remote field sites. The weight and size of the Matrice 350 was not an issue at the Lemon Creek glacier or Bagley Basin, where we were able to transport the UAV to the field site by either car or helicopter. Access to the Easton glacier on Mt. Baker, however, required carrying all the gear needed for the UAV mapping survey along an 8-mile out-and-back trail with 2650 ft of elevation gain. This trek would have been much more difficult if carrying the Matrice 350 and its heavier batteries.

The batteries for the Mavic 3M (DJI Mavic 3 Series Intelligent Flight Battery) weigh 335.5 g, they store 77 Wh of energy, and they have a MSRP of $209 each. The batteries for the Matrice 350 (TB 65 Intelligent Flight Battery) weigh 1.35 kg, they store 263.2 Wh of energy, and they have a MSRP of $700 each. The larger Matrice 350 batteries enable it to have a longer maximum flight time when compared to the Mavic 3M (55 min vs. 43 min), however it needs two batteries to operate. In contrast, the Mavic 3M only needs one battery to operate. This results in increased weight, additional cost to purchase a sufficient number of batteries, and an increased amount of electricity needed to charge the batteries. At the Lemon Creek glacier, all UAV batteries were charged with a gas-powered generator. The increased energy needed to charge the Matrice 350 batteries resulted in increased fuel consumption. Furthermore, since the energy of the Matrice 350 batteries is 263.2 Wh, they cannot be carried onto an airplane according to airline regulations.

Both UAV systems were able to produce orthomosaic models of the surface of the Lemon Creek glacier. The Mavic 3M produced an RGB orthomosaic image and a 4-band multispectral composite orthomosaic image, and the Micasense camera produced a 10-band multispectral composite orthomosaic image. Visual artifacts are present in all the orthomosaics produced. Since such a large area of the Lemon Creek glacier was mapped, both UAVs were flown for several hours over a three-day period to collect the necessary imagery. During these flights, lighting conditions and cloud cover varied, leading to

variations in exposure and regions of the orthomosaic that were more shadowed than others. The Mavic 3M RGB orthomosaic has a small region in the western part of the image where the cameras were unable to align during the image alignment step within Agisoft Metashape Pro, resulting in a small gap with no data. The Micasense orthomosaic suffers from striping artifacts that are oriented along parallel flight lines. This striping is likely present because the Micasense camera was not attached to the M350 with a gimbal but was instead hard mounted to the bottom of the drone. The Mavic 3M, in contrast, comes equipped with a gimbal, allowing its sensor to point nadir during flight.

Similar results were achieved when classifying red snow algae in the southern region of the Lemon Creek glacier using both camera systems. When the ORG index was applied to this region, a threshold value of 1.08 applied to the Micasense orthomosaic classified a 3.36% greater area than a threshold value of 0.65 applied to the Mavic 3M orthomosaic. When a random forest supervised classification algorithm was applied to this region, a 17.4% greater area was classified as red snow algae in the Micasense orthomosaic than in the Mavic 3M orthomosaic. These results reveal that the fewer spectral bands of the Mavic 3M camera system do not significantly affect its performance when compared to the Micasense camera system.

The RGB orthomosaics and DEMs of Bagley Basin, produced by the Mavic 3M mapping campaigns throughout the early 2023 summer season, proved to be capable of monitoring small scale features, such as the change in suncup morphology on the snow surface. Suncups from a snow-covered surface to the west of Upper Bagley Lake got progressively larger as the season progressed, until the snow-cover completely melted out of the basin.

The RGB camera on the Mavic 3M was able to produce high resolution orthomosaic images and DEMs. When a random forest supervised classification was performed on the RGB orthomosaic, it was able to accurately classify glacier surface features, including snow, ice, rock and heavy debris, and crevasses. The RGB orthomosaic was input to the random forest classifier instead of the multispectral orthomosaic because the Mavic 3M lacks a band in the blue wavelengths, which is needed to accurately differentiate between blue glacier ice and snow. The inclusion of a blue band would have likely increased the accuracy of supervised classification of glacier surface features since the reflectance measured by the multispectral sensors is more accurate than the RGB camera.

5. Conclusions

The Mavic 3M is a useful, low-cost UAV that can be utilized for a wide variety of cryospheric research. This UAV is considerably cheaper than alternative systems, such as the Matrice 350 and Micasense camera, making it more accessible to a wider range of researchers. The Mavic 3M is significantly lighter and smaller than the Matrice 350, making it a much more portable option that is easy to transport into the field. When classifying red snow algae on snow surfaces, the two systems produce similar results when utilizing spectral indices or a random forest supervised classification. The UAV can also visualize small-scale features such as suncups. The RGB camera is capable of producing high resolution orthomosaics and DEMs. The RGB orthomosaic can be input to a random forest supervised classification algorithm to classify glacier surface features with high accuracy.

The applicability of this UAV for cryospheric research is limited by the number of spectral bands, which is fewer than many of the alternatives, such as the Micasense cameras. The lack of a blue band, specifically, makes it more difficult to classify glacier surface features, such as snow and ice.

Supplementary Materials: The following supporting information can be downloaded at: https://www.mdpi.com/article/10.3390/rs16193662/s1.

Author Contributions: Conceptualization, C.F.R. and A.L.K.; methodology, C.F.R. and A.L.K.; validation, C.F.R.; formal analysis, C.F.R.; investigation, C.F.R. and A.L.K.; resources, A.L.K.; data curation, C.F.R.; writing—original draft preparation, C.F.R.; writing—review and editing, A.L.K.; visualization,

C.F.R.; supervision, A.L.K.; project administration, A.L.K.; funding acquisition, C.F.R. and A.L.K. All authors have read and agreed to the published version of the manuscript.

Funding: This research was funded by National Aeronautics and Space Administration (NASA), grant number #80NSSC21K1166, National Science Foundation (NSF) Arctic Observing Network, award #2218834, and Western Washington University Graduate Research and Creative Opportunities Grant, award #GGR05A.

Data Availability Statement: All data used in this study is available upon request.

Acknowledgments: DEMs used during UAV flight missions to enable terrain follow functionality provided by the Polar Geospatial Center under NSF-OPP awards 1043681, 1559691, 1542736, 1810976, and 2129685.

Conflicts of Interest: The authors declare no conflicts of interest. The funders had no role in the design of the study; in the collection, analyses, or interpretation of data; in the writing of the manuscript; or in the decision to publish the results.

Appendix A

Table A1. Flight parameters and the associated ground resolution of the orthomosaics for each flight conducted in this study.

UAV and Sensor	Location	Date	Flight Altitude	Front Overlap	Side Overlap	Terrain Follow	Ground Resolution (RGB Orthomosaic)	Ground Resolution (Multispectral Orthomosaic)
Mavic 3M	Bagley Basin	8 June 2023	70 m	80%	80%	Real-time terrain follow	2.1 cm/pixel	3.6 cm/pixel
Mavic 3M	Bagley Basin	26 June 2023	80 m	85%	75%	Real-time terrain follow	2.5 cm/pixel	4.2 cm/pixel
Mavic 3M	Bagley Basin	5 July 2023	70 m	85%	85%	Real-time terrain follow	2.1 cm/pixel	3.5 cm/pixel
Mavic 3M	Bagley Basin	10 July 2023	70 m	80%	80%	Real-time terrain follow	1.8 cm/pixel	3.1 cm/pixel
Mavic 3M	Bagley Basin	13 July 2023	70 m	80%	80%	EarthDEM	1.8 cm/pixel	3.1 cm/pixel
Mavic 3M	Bagley Basin	17 July 2023	70 m	80%	80%	EarthDEM	1.9 cm/pixel	3.2 cm/pixel
Mavic 3M	Easton glacier	20 July 2023	80 m	80%	80%	EarthDEM	2.4 cm/pixel	4.0 cm/pixel
Mavic 3M	Easton glacier	1 August 2023	80 m	80%	80%	EarthDEM	2.7 cm/pixel	4.5 cm/pixel
Mavic 3M	Easton Glacier	13 August 2023	80 m	80%	80%	EarthDEM	2.4 cm/pixel	4.0 cm/pixel
Mavic 3M	Lemon Creek glacier	21 August 2023 through 23 August 2023	80 m	80%	75%	ArcticDEM	1.8 cm/pixel	3.1 cm/pixel
Matrice 350 + Micasense	Lemon Creek glacier	21 August through 23 August 2023	70 m	–	75%	ArcticDEM	–	5.0 cm/pixel
Mavic 3M	Easton glacier	8 September 2023	80 m	80%	80%	EarthDEM	2.4 cm/pixel	4.0 cm/pixel

References

1. Meredith, M.; Sommerkorn, M.; Cassotta, S.; Derksen, C.; Ekaykin, A.; Hollowed, A.; Kofinas, G.; Mackintosh, A.; Melbourne-Thomas, J.; Muelbert, M.M.C.; et al. Polar Regions. IPCC Special Report on the Ocean and Cryosphere in a Changing Climate. 2019. Available online: https://www.ipcc.ch/site/assets/uploads/sites/3/2019/11/07_SROCC_Ch03_FINAL.pdf (accessed on 27 July 2024).
2. Dietz, A.J.; Kuenzer, C.; Gessner, U.; Dech, S. Remote Sensing of Snow—A Review of Available Methods. *Int. J. Remote Sens.* **2012**, *33*, 4094–4134. [CrossRef]
3. Gaffey, C.; Bhardwaj, A. Applications of Unmanned Aerial Vehicles in Cryosphere: Latest Advances and Prospects. *Remote Sens.* **2020**, *12*, 948. [CrossRef]
4. Tovar-Sánchez, A.; Román, A.; Roque-Atienza, D.; Navarro, G. Applications of Unmanned Aerial Vehicles in Antarctic Environmental Research. *Sci. Rep.* **2021**, *11*, 21717. [CrossRef]
5. Bhardwaj, A.; Sam, L.; Akanksha; Martín-Torres, F.J.; Kumar, R. UAVs as Remote Sensing Platform in Glaciology: Present Applications and Future Prospects. *Remote Sens. Environ.* **2016**, *175*, 196–204. [CrossRef]
6. Healy, S.M.; Khan, A.L. Albedo Change from Snow Algae Blooms Can Contribute Substantially to Snow Melt in the North Cascades, USA. *Commun. Earth Environ.* **2023**, *4*, 142. [CrossRef]
7. Rossini, M.; Garzonio, R.; Panigada, C.; Tagliabue, G.; Bramati, G.; Vezzoli, G.; Cogliati, S.; Colombo, R.; Di Mauro, B. Mapping Surface Features of an Alpine Glacier through Multispectral and Thermal Drone Surveys. *Remote Sens.* **2023**, *15*, 3429. [CrossRef]

8. Bühler, Y.; Adams, M.S.; Bösch, R.; Stoffel, A. Mapping Snow Depth in Alpine Terrain with Unmanned Aerial Systems (UASs): Potential and Limitations. *Cryosphere* **2016**, *10*, 1075–1088. [CrossRef]
9. Healy, S.M.; Khan, A.L. Mapping Glacier Ablation with a UAV in the North Cascades: A Structure-from-Motion Approach. *Front. Remote Sens.* **2022**, *2*, 764765. [CrossRef]
10. Kol, E.; Taylor, W.R. The Snow and Ice Algae of Alaska. *Smithson. Misc. Collect.* **1942**, *101*, 1–36.
11. Skiles, S.M.; Flanner, M.; Cook, J.M.; Dumont, M.; Painter, T.H. Radiative Forcing by Light-Absorbing Particles in Snow. *Nat. Clim. Chang.* **2018**, *8*, 964–971. [CrossRef]
12. Khan, A.L.; Dierssen, H.M.; Scambos, T.A.; Höfer, J.; Cordero, R.R. Spectral Characterization, Radiative Forcing and Pigment Content of Coastal Antarctic Snow Algae: Approaches to Spectrally Discriminate Red and Green Communities and Their Impact on Snowmelt. *Cryosphere* **2021**, *15*, 133–148. [CrossRef]
13. Chevrollier, L.-A.; Cook, J.M.; Halbach, L.; Jakobsen, H.; Benning, L.G.; Anesio, A.M.; Tranter, M. Light Absorption and Albedo Reduction by Pigmented Microalgae on Snow and Ice. *J. Glaciol.* **2022**, *69*, 333–341. [CrossRef]
14. Dial, R.J.; Ganey, G.Q.; Skiles, S.M. What Color Should Glacier Algae Be? An Ecological Role for Red Carbon in the Cryosphere. *FEMS Microbiol. Ecol.* **2018**, *94*, fiy007. [CrossRef]
15. Huovinen, P.; Ramírez, J.; Gómez, I. Remote Sensing of Albedo-Reducing Snow Algae and Impurities in the Maritime Antarctica. *ISPRS J. Photogramm. Remote Sens.* **2018**, *146*, 507–517. [CrossRef]
16. Ganey, G.Q.; Loso, M.G.; Burgess, A.B.; Dial, R.J. The Role of Microbes in Snowmelt and Radiative Forcing on an Alaskan Icefield. *Nat. Geosci.* **2017**, *10*, 754–759. [CrossRef]
17. Painter, T.H.; Duval, B.; Thomas, W.H.; Mendez, M.; Heintzelman, S.; Dozier, J. Detection and Quantification of Snow Algae with an Airborne Imaging Spectrometer. *Appl. Environ. Microbiol.* **2001**, *67*, 5267–5272. [CrossRef]
18. Takeuchi, N.; Dial, R.; Kohshima, S.; Segawa, T.; Uetake, J. Spatial Distribution and Abundance of Red Snow Algae on the Harding Icefield, Alaska Derived from a Satellite Image. *Geophys. Res. Lett.* **2006**, *33*, L21502. [CrossRef]
19. Hisakawa, N.; Quistad, S.D.; Hester, E.R.; Martynova, D.; Maughan, H.; Sala, E.; Gavrilo, M.V.; Rohwer, F. Metagenomic and Satellite Analyses of Red Snow in the Russian Arctic. *PeerJ* **2015**, *3*, e1491. [CrossRef]
20. Engstrom, C.B.; Williamson, S.N.; Gamon, J.A.; Quarmby, L.M. Seasonal Development and Radiative Forcing of Red Snow Algal Blooms on Two Glaciers in British Columbia, Canada, Summer 2020. *Remote Sens. Environ.* **2022**, *280*, 113164. [CrossRef]
21. Engstrom, C.B.; Quarmby, L.M. Satellite Mapping of Red Snow on North American Glaciers. *Sci. Adv.* **2023**, *9*, eadi3268. [CrossRef]
22. Gray, A.; Krolikowski, M.; Fretwell, P.; Convey, P.; Peck, L.S.; Mendelova, M.; Smith, A.G.; Davey, M.P. Remote Sensing Reveals Antarctic Green Snow Algae as Important Terrestrial Carbon Sink. *Nat. Commun.* **2020**, *11*, 2527. [CrossRef]
23. Gray, A.; Krolikowski, M.; Fretwell, P.; Convey, P.; Peck, L.S.; Mendelova, M.; Smith, A.G.; Davey, M.P. Remote Sensing Phenology of Antarctic Green and Red Snow Algae Using WorldView Satellites. *Front. Plant Sci.* **2021**, *12*, 671981. [CrossRef]
24. Bash, E.; Moorman, B.; Gunther, A. Detecting Short-Term Surface Melt on an Arctic Glacier Using UAV Surveys. *Remote Sens.* **2018**, *10*, 1547. [CrossRef]
25. McNeil, C.; O'Neel, S.; Loso, M.; Pelto, M.; Sass, L.; Baker, E.H.; Campbell, S. Explaining Mass Balance and Retreat Dichotomies at Taku and Lemon Creek Glaciers, Alaska. *J. Glaciol.* **2020**, *66*, 530–542. [CrossRef]
26. RGI Consortium. Randolph Glacier Inventory—A Dataset of Global Glacier Outlines, Version 7. 2023. Available online: https://nsidc.org/data/nsidc-0770/versions/7 (accessed on 20 May 2024).
27. Leffler, R.; Horvitz, A.; Downs, R.; Changery, M.; Redmond, K.T.; Taylor, G. Evaluation of a National Seasonal Snowfall Record at the Mount Baker, Washington, Ski Area. *Natl. Weather Dig.* **2022**, *25*, 15–20.
28. Pelto, M.S. The Annual Balance of North Cascade Glaciers, Washington, U.S.A., Measured and Predicted Using an Activity-Index Method. *J. Glaciol.* **1988**, *34*, 194–199. [CrossRef]
29. Pelto, M.; Brown, C. Mass Balance Loss of Mount Baker, Washington Glaciers 1990–2010. *Hydrol. Process.* **2012**, *26*, 2601–2607. [CrossRef]
30. DJI DJI Mavic 3M User Manual v1.0. 2022. Available online: https://dl.djicdn.com/downloads/DJI_Mavic_3_Enterprise/20221216/DJI_Mavic_3M_User_Manual-EN.pdf (accessed on 6 March 2024).
31. Agisoft LLC Agisoft Metashape User Manual: Professional Edition, Version 2.1. 2024. Available online: https://www.agisoft.com/pdf/metashape-pro_2_1_en.pdf (accessed on 29 April 2024).